Locating and confirming the C–H stretch bands of the halide–acetylene anion complexes using argon predissociation spectroscopy

4 AUTHORS, INCLUDING:

Duncan A Wild
University of Western Australia
49 PUBLICATIONS **668** CITATIONS

SEE PROFILE

Locating and confirming the C–H stretch bands of the halide–acetylene anion complexes using argon predissociation spectroscopy

D.A. Wild, Z.M. Loh, R.L. Wilson, E.J. Bieske *

School of Chemistry, University of Melbourne, Parkville 3010, Vic., Australia

Received 6 November 2002; in final form 19 December 2002

Abstract

Infrared spectra of $Cl^-–C_2H_2 \cdot Ar$, $Br^-–C_2H_2 \cdot Ar$, and $I^-–C_2H_2 \cdot Ar$ are recorded in the C–H stretch region by monitoring production of $X^-–C_2H_2$ photofragments. Each spectrum exhibits a single band corresponding to the vibration of a hydrogen-bonded C–H unit ($\nu_{HB} = 2882, 2982, 3075$ cm^{-1} for $Cl^-–C_2H_2 \cdot Ar$, $Br^-–C_2H_2 \cdot Ar$, $I^-–C_2H_2 \cdot Ar$, respectively). Marked differences between the spectra of $Cl^-–C_2H_2 \cdot Ar$ and $Cl^-–C_2H_2$ are attributable to the strong $Cl^-–HCCH$ bond which prevents cold $Cl^-–C_2H_2$ complexes from dissociating following absorption of an infrared photon. The evidence suggests that addition of the first few Ar solvent atoms has a minor influence on the C–H stretch vibrations of the halide–acetylene complexes.
© 2003 Elsevier Science B.V. All rights reserved.

1. Introduction

Gas-phase infrared spectroscopic studies of negatively charged complexes and clusters offer a unique opportunity to explore the nature of hydrogen bonds between neutral 'solvent' molecules and anion 'solute' atoms or molecules. Our investigations have focussed on clusters consisting of acetylene solvent molecules attached to solute halide anions. So far, we have reported infrared spectra of size-selected $Cl^-–(C_2H_2)_n$ ($n = 1–9$) [1], $Br^-–(C_2H_2)_n$ ($n = 1–8$) [2,3], and $I^-–(C_2H_2)_n$ ($n = 1–4$) [4] clusters. Mostly, the spectra are ap-

pealingly simple, and are consistent with the smaller clusters having structures in which equivalent C_2H_2 ligands are attached to the central halide anion by linear hydrogen bonds. For clusters containing more than 6–8 acetylene ligands, the first solvation shell is filled and acetylene units begin to occupy the second shell.

The spectra were obtained by irradiating mass-selected complexes with tuneable IR light in the region of the C–H stretch vibrations while monitoring production of charged photofragments. Energy deposited in the high frequency C–H stretch vibrational mode migrates into the softer intermolecular modes leading to cluster fragmentation. Since photon absorption is inferred from the production of fragment ions, one limitation of this *action* technique is that it is usually only useful

---

* Corresponding author. Fax: +61-3-9347-5180.
E-mail address: evanjb@unimelb.edu.au (E.J. Bieske).

for probing transitions terminating above the clusters' dissociation threshold. Recording spectra that faithfully reflect the fundamental vibrational transitions of the complexes by detecting charged photofragments is more likely to be a problem for the $Cl^- - C_2H_2$, $Br^- - C_2H_2$, and $I^- - C_2H_2$ dimers than for the larger clusters, since the energy required to detach a C_2H_2 unit is expected to decline as the clusters become larger.

Of the three dimers, $Cl^- - C_2H_2$ is expected to have the largest dissociation energy. In the original $Cl^- - C_2H_2$ spectrum two bands were observed, both shifted to lower energy from the v_3 antisymmetric C–H stretch band of the bare C_2H_2 molecule. The stronger band at 2938 cm^{-1} was originally assigned to the stretching vibration of the H-bonded C–H group (v_{HB}), while the weaker peak at 2810 cm^{-1} was assigned to the $v_2 + v_5$ combination band. These assignments were tentative and it was suggested that a $Cl^- - C_2H_2$ dimer possessing a single quantum of v_{HB} may not have sufficient energy to dissociate and that the observed features may be hot bands associated with vibrationally excited clusters. This proposal is supported by recent theoretical work. On the basis of rovibrational calculations performed using an ab initio potential energy surface computed at the MP2(full)/aug-cc-pVTZ level, Meuwly et al. [5] predicted a v_{HB} frequency of 2843 cm^{-1} and binding energy of 3512 cm^{-1} (with respect to $Cl^- + C_2H_2$ fragments). More recently, on the basis of large scale CCSD(T) calculations, Botschwina and Oswald [6] predicted a v_{HB} frequency of 2877 cm^{-1} and a dissociation energy of 3600 cm^{-1}.

In the current work we have recorded infrared spectra of $Cl^- - C_2H_2 \cdot Ar$, $Br^- - C_2H_2 \cdot Ar$, and $I^- - C_2H_2 \cdot Ar$ by monitoring production of $X^- - C_2H_2$ photofragments (Ar loss channel). The trick of adding an easily detached 'spy' or 'messenger' atom to spectroscopically probe the core ion cluster was initially devised to investigate protonated water clusters [7]. The technique has recently been used to great effect by Johnson and co-workers [8–10] for elucidating the vibrational properties of the halide–water and solvated electron complexes.

Spectra of the halide–acetylene argon solvated complexes should provide a reliable picture of the vibrational properties of the core $X^- - C_2H_2$ anion complexes since the attached Ar atom is expected to have a minor perturbative effect and should be dislodged easily following deposition of energy into a C–H stretch mode. Although the Ar binding energies for the $X^- - C_2H_2 \cdot Ar$ complexes are unknown, they are probably similar to the binding energies of an Ar atom to the Cl^-, Br^-, and I^- halides, which, on the basis of empirical potential energy curves derived from ZEKE spectra [11,12] have been determined as 494, 418, and 352 cm^{-1}.

2. Experimental methods

Infrared spectra of mass-selected $Cl^- - C_2H_2 \cdot Ar$, $Br^- - C_2H_2 \cdot Ar$, and $I^- - C_2H_2 \cdot Ar$ complexes were obtained by monitoring the production of charged $X^- - C_2H_2$ photofragments as the infrared wavelength was scanned over the C–H stretching region. The experimental set-up is a tandem mass spectrometer equipped with an ion source designed to generate cooled cluster ions. The mass spectrometer is comprised of a primary quadrupole mass filter for selection of the parent $X^- - C_2H_2 \cdot Ar$ ions, an octopole ion guide where the ions are overlapped with the counter-propagating output of a pulsed tuneable IR radiation source (Continuum Mirage 3000 OPO, ≈0.02 cm^{-1} bandwidth), and a second quadrupole mass filter tuned to the mass of the daughter $X^- - C_2H_2$ ions. Photofragment ions were sensed with a channel plate detector. Wavelength calibration was achieved by using a wavemeter (New Focus 7711) to measure the wavelength of the signal output from the first stage of the optical parametric oscillator, and the 532 nm output of the seeded Nd:YAG laser.

The $X^- - C_2H_2 \cdot Ar$ complexes were produced in an electron beam crossed supersonic expansion of a 1:49:50 ratio of acetylene/helium/argon seeded with traces of the appropriate halide ion precursor (CCl_4, CH_2Br_2, and CH_3I). Optimum complex formation required a relatively small separation between the nozzle orifice and the electron impact zone, suggesting that C_2H_2 molecules and Ar atoms accrete about halide ions through three-body association reactions in the initial part of the

expansion. Further details of the experimental arrangement can be found in [1,4].

3. Results and discussion

3.1. Overview

The halide–acetylene complexes have been thoroughly characterised in a series of ab initio studies, most recently by Botschwina and co-workers [6,13] through large-scale CCSD(T) calculations, coupled with the determination of anharmonic stretching frequencies using a stretch-only Hamiltonian. All the calculations predict that the complexes have linear equilibrium structures, with a substantial energy barrier separating the two equivalent H-bonded minima.

When an acetylene molecule is attached to a halide anion, the symmetric (v_1) and antisymmetric (v_3) C–H stretch vibrations are transformed into vibrations predominantly involving motion of the H-bonded C–H bond (v_{HB}) and free C–H bond (v_F). The v_{HB} vibration, which is strongly infrared active, is displaced to lower frequency with respect to the C_2H_2 v_1 and v_3 vibrational modes, with the magnitude of the red-shift correlating with the strength of the H-bond. The red-shifts, which decrease in the order $Cl^- > Br^- > I^-$, are symptomatic of slight proton transfer from the HCC^- anion, whose proton affinity (PA) is 1580 kJ/mol, [14] towards the Cl^- (PA = 1395 kJ/mol [15]), Br^- (PA = 1353.5 kJ/mol [16]) and I^- (PA = 1315 kJ/mol [17]) halide anions. For all three complexes, v_F is predicted to occur between the free C_2H_2 v_1 and v_3 vibrational modes, and to have an infrared intensity of several orders of magnitude less than v_{HB} [6,13].

In the following sections we explore the effects of argon solvation on the vibrational properties of the halide–acetylene complexes, considering, in turn, the spectra of $Cl^-–C_2H_2 \cdot Ar_n$ ($n = 0–2$), $Br^-–C_2H_2 \cdot Ar_n$ ($n = 0–1$) and $I^-–C_2H_2 \cdot Ar_n$ ($n = 0–1$).

3.2. The $Cl^-–C_2H_2 \cdot Ar_n$ ($n=0–2$) complexes

The $Cl^-–C_2H_2 \cdot Ar_n$ ($n = 0–2$) spectra, recorded by monitoring $Cl^-–C_2H_2$ photofragments, are displayed in Fig. 1. Spectroscopic data for the

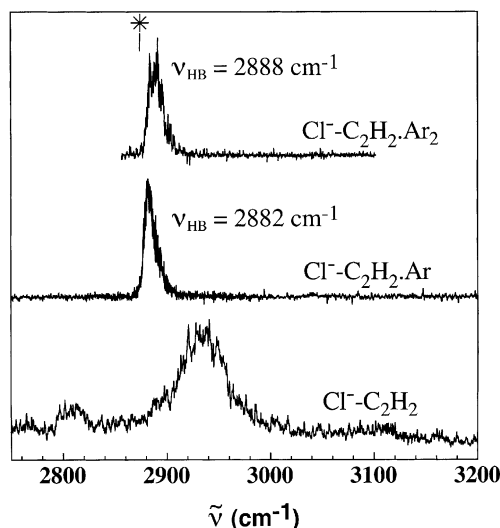Fig. 1. Infrared spectra of $Cl^- – C_2H_2 \cdot Ar_n$ ($n = 0–2$). The calculated v_{HB} frequency from [6] is marked by an asterisk.

observed transitions are listed in Table 1. The spectra of $Cl^-–C_2H_2 \cdot Ar$ and $Cl^-–C_2H_2 \cdot Ar_2$ are very similar, each containing a single compact band, centred at 2882 and 2888 cm^{-1} respectively, that can be convincingly associated with the v_{HB} C–H stretch mode of a core, linear $Cl^-–C_2H_2$ complex. The similarity of the $n = 1$ and 2 spectra strongly suggests that addition of one or two Ar atoms has a minor effect on the vibrational properties of the $Cl^-–C_2H_2$ core. Linear extrapolation of the v_{HB} frequencies for the $Cl^-–C_2H_2 \cdot Ar_n$ $n = 1–2$ complexes yields an estimated frequency of 2876 cm^{-1} for the v_{HB} vibration of the bare $Cl^-–C_2H_2$ complex, in excellent agreement with the prediction of Botschwina and Oswald (2877 cm^{-1} [6]) and close to the prediction of Meuwly et al. (2843 cm^{-1} [5]). For $Cl^-–C_2H_2 \cdot Ar$, we searched in vain for the weak v_F transition, which is predicted to occur in the 3300–3400 cm^{-1} range.

The $Cl^-–C_2H_2$ spectrum, which was obtained by monitoring Cl^- fragments, contains two broad peaks, neither of which corresponds to the bands observed for $Cl^-–C_2H_2 \cdot Ar$ and $Cl^-–C_2H_2 \cdot Ar_2$. While it might be suspected that the differences arise from the effects of the Ar solvation on the vibrational properties of the core $Cl^-–C_2H_2$ complex, a more likely explanation is that cold

Table 1
Experimental and theoretical data for ν_{HB} transitions of $Cl^- - C_2H_2 \cdot Ar_n$ ($n = 0–2$), $Br^- - C_2H_2 \cdot Ar_n$ ($n = 0–1$) and $Br^- - C_2H_2 \cdot Ar_n$ ($n = 0–1$)

Species	ν_{HB} Exp.[a]	Bandwidth	ν_{HB} Calc.
$Cl^- - C_2H_2$	2938(10)	50	2877[b], 2843[c]
$Cl^- - C_2H_2 \cdot Ar$	2882(2)	12	
$Cl^- - C_2H_2 \cdot Ar_2$	2888(2)	13	
$Br^- - C_2H_2$	2981.28(8)		2964[d]
$Br^- - C_2H_2 \cdot Ar$	2982(2)	10	
$I^- - C_2H_2$	3074(3)		3050[d]
$I^- - C_2H_2 \cdot Ar$	3075(2)	8	

Units for band positions and widths are cm^{-1}. Estimated uncertainties for band positions are given in brackets.
[a] Wavenumbers for argon solvated complexes correspond to ν_{HB} band maxima. Experimental data for $Cl^- - C_2H_2$, $Br^- - C_2H_2$ and $I^- - C_2H_2$ are taken from [1,3,4].
[b] Ref. [6].
[c] Ref. [5].
[d] Ref. [13].

$Cl^- - C_2H_2$ complexes do not dissociate following the absorption of a single 3 μm photon and that the bands are associated with hot band transitions terminating at levels lying above the dissociation threshold. Support for this view is provided by recent calculations that predict that the dissociation energy of $Cl^- - C_2H_2$ ($D_0 = 3600$ cm^{-1} [6]) lies well above ν_{HB}. It seems most plausible that the stronger band in the $Cl^- - C_2H_2$ spectrum (at 2938 cm^{-1}) corresponds to overlapping sequence bands of the type $(\nu_{HB} + m\nu_s + n\nu_b) \leftarrow (m\nu_s + n\nu_b)$ involving the intermolecular stretch mode (ν_s) and intermolecular bend mode (ν_b). Due to positive cross anharmonicity between ν_{HB} and the intermolecular modes, these transitions occur to higher energy from ν_{HB} [6]. On the basis of calculated ν_s and ν_b frequencies (153 and 146 cm^{-1}; [6]), $m + n$ would need to exceed 5 or 6 for the upper level of the transition to lie above the $Cl^- + C_2H_2$ dissociation asymptote.

It is interesting to consider the new $Cl^- - C_2H_2 \cdot Ar$ and $Cl^- - C_2H_2 \cdot Ar_2$ spectra in the context of the previously reported spectra of the larger $Cl^- - (C_2H_2)_n$ clusters [1]. It was deduced that clusters containing up to 8 C_2H_2 molecules adopt structures in which equivalent C_2H_2 ligands are bound by linear H-bonds to the Cl^- core (although the $n = 7$ and 8 clusters also possess isomers with C_2H_2 ligands in the second solvation shell). The hydrogen bonds become progressively weaker as the clusters become larger so that the ν_{HB} band

moves back towards the ν_3 transition of the free C_2H_2 molecule. In Fig. 2, the ν_{HB} band positions for inner solvation shell C_2H_2 ligands of the $Cl^- - (C_2H_2)_n$ clusters ($n = 1–8$) are plotted as a function of n. It can be seen that whereas the ν_{HB} band of $Cl^- - C_2H_2 \cdot Ar$ occurs at a frequency that can be anticipated from the ν_{HB} frequencies of the larger $Cl^- - (C_2H_2)_n$ ($n = 2–8$) clusters, neither of the two bands observed for the bare $Cl^- - C_2H_2$ dimer have frequencies that fit the trend established for the larger clusters.

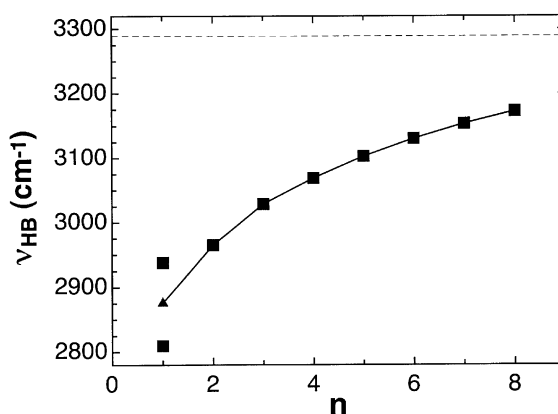Fig. 2. The ν_{HB} band positions for inner solvation shell C_2H_2 ligands of $Cl^- - (C_2H_2)_n$ ($n = 1–8$) plotted as a function of n (■). The ν_{HB} band position for $Cl^- - C_2H_2 \cdot Ar$ is also shown (▲). The dotted line indicates the ν_3 frequency of the bare C_2H_2 molecule (3288.7 cm^{-1} [19]).

3.3. The $Br^- – C_2H_2 \cdot Ar_n$ ($n = 0–1$) complexes

Spectra of $Br^- – C_2H_2$ and $Br^- – C_2H_2 \cdot Ar$ in the ν_{HB} region are shown in Fig. 3, while data for the observed transitions are listed in Table 1. It can be seen that whereas the $Br^- – C_2H_2 \cdot Ar$ spectrum exhibits as single compact band, the spectrum of $Br^- – C_2H_2$ is more complex, featuring a series of sharp peaks protruding from a broad hump. Previously, we have assigned the lowest energy peak as the P-branch head of the ν_{HB} transition and the series of peaks extending to higher energy as the heads of hot band sequence transitions involving the intermolecular modes, having the form $(\nu_{HB} + m\nu_s + n\nu_b) \leftarrow (m\nu_s + n\nu_b)$.

As described in [3], the $Br^- – C_2H_2$ spectrum exhibits rotationally resolved features, enabling structural and energetic data to be deduced. Between the two lowest energy sharp peaks in the $Br^- – C_2H_2$ spectrum, there are 7 resolved rovibrational lines that have been assigned as the ν_{HB} R(27)–R(34) transitions (these lines are not visible in the compressed spectrum shown in Fig. 3). The unresolved P branch exhibits an onset at P(29) and reaches a head at P(53). Lower J lines in the P and R branches are absent from the vibrational

Fig. 3. Infrared spectra of $Br^- – C_2H_2$, $Br^- – C_2H_2 \cdot Ar$, $I^- – C_2H_2$ and $I^- – C_2H_2 \cdot Ar$. Calculated ν_{HB} frequencies for $Br^- – C_2H_2$ and $I^- – C_2H_2$ from [13] are marked by asterisks.

predissociation spectrum because the upper levels with $J' < 28$ lie below the $Br^- + C_2H_2$ dissociation asymptote. Analysis of the rovibrational structure shows that the origin of the ν_{HB} band occurs at 2981.28 cm^{-1}, slightly below the dissociation energy (3020 ± 3 cm^{-1}).

The new $Br^- – C_2H_2 \cdot Ar$ data support the earlier interpretation of the $Br^- – C_2H_2$ spectrum. The $Br^- – C_2H_2 \cdot Ar$ ν_{HB} band has a maximum at 2982 cm^{-1}, within 1 cm^{-1} of the previously deduced ν_{HB} origin for $Br^- – C_2H_2$, and very close to the ν_{HB} frequency calculated by Botschwina and Stoll (2964 cm^{-1}; [13]). The ν_{HB} band of $Br^- – C_2H_2 \cdot Ar$ is relatively compact (fwhm ≈ 10 cm^{-1}) suggesting that the $(\nu_{HB} + m\nu_s + n\nu_b) \leftarrow (m\nu_s + n\nu_b)$ hot bands, which are so prominent in the $Br^- – C_2H_2$ spectrum, are largely suppressed. The absence of hot bands is to be expected, as there will be an upper bound on the clusters' internal energy, corresponding to the binding energy of the Ar atom. Assuming $\nu_s = 117$ cm^{-1} and $\nu_b = 132$ cm^{-1} (harmonic values calculated in [13]), and that the energy required to remove an Ar atom from $Br^- – C_2H_2 \cdot Ar$ is the same as it is for $Br^- – Ar$ (418 cm^{-1} [11]), the $Br^- – C_2H_2 \cdot Ar$ complexes can contain at the most 3–4 quanta distributed between the intermolecular stretch and bend modes of the $Br^- – C_2H_2$ core.

3.4. The $I^- – C_2H_2 \cdot Ar_n$ ($n = 0–1$) complexes

Spectra of $I^- – C_2H_2$ and $I^- – C_2H_2 \cdot Ar$ are also shown in Fig. 3. Data for the transitions are listed in Table 1. The situation for $I^- – C_2H_2$ is very similar to that of $Br^- – C_2H_2$, although for $I^- – C_2H_2$, ν_{HB} is predicted to lie well above the dissociation energy ($D_0 = 2450$ cm^{-1} [13]). The maximum of the $I^- – C_2H_2 \cdot Ar$ ν_{HB} band (3075 cm^{-1}) occurs between the two lowest energy sharp peaks in the $I^- – C_2H_2$ spectrum (which lie at 3071.8 and 3079.0 cm^{-1}) and corresponds very well with the value calculated by Botschwina and Stoll (3050 cm^{-1} [13]). As in the case of $Br^- – C_2H_2 / Br^- – C_2H_2 \cdot Ar$ the $(\nu_{HB} + m\nu_s + n\nu_b) \leftarrow (m\nu_s + n\nu_b)$ hot bands, which are prominent in the spectrum of $I^- – C_2H_2$, are suppressed in the spectrum of $I^- – C_2H_2 \cdot Ar$, due to limitations on the internal energy of the Ar solvated complex.
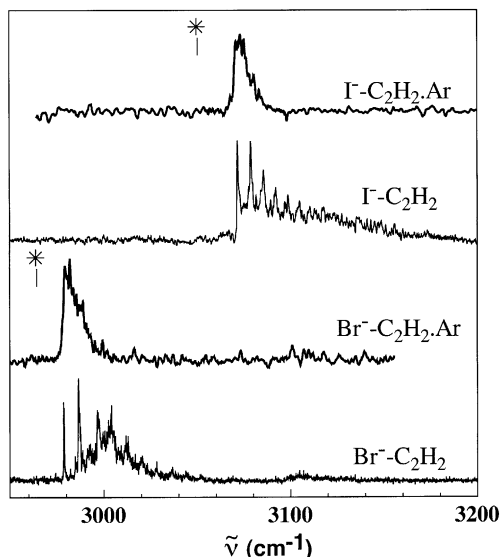
4. Summary and conclusion

The evidence suggests that the mid-infrared spectra of the $Cl^- – C_2H_2 \cdot Ar$, $Br^- – C_2H_2 \cdot Ar$, and $I^- – C_2H_2 \cdot Ar$ clusters provide reliable information on the ν_{HB} frequencies of the core halide–acetylene complexes. In the case of $Br^- – C_2H_2 \cdot Ar$ and $I^- – C_2H_2 \cdot Ar$, the maxima of the ν_{HB} bands fall within a few cm^{-1} of the ν_{HB} bands of the bare $Br^- – C_2H_2$ and $I^- – C_2H_2$ complexes. Marked differences between the spectra of $Cl^- – C_2H_2 \cdot Ar_n$ ($n = 1,2$) and $Cl^- – C_2H_2$ are attributable to the strong $Cl^- – HCCH$ bond which prevents cold $Cl^- – C_2H_2$ complexes from dissociating following absorption of a single infrared photon. Vibrational predissociation spectroscopy is more successful in directly revealing the vibrational properties of the bare $Br^- – C_2H_2$ and $I^- – C_2H_2$ complexes where weaker H-bonds allow vibrationally cold complexes to dissociate following excitation of the ν_{HB} vibration (although for $Br^- – C_2H_2$ this only occurs for complexes possessing $\approx 40 \ cm^{-1}$ of rotational energy).

The maxima of the $Cl^- – C_2H_2 \cdot Ar$, $Br^- – C_2H_2 \cdot Ar$ and $I^- – C_2H_2 \cdot Ar$ bands correspond very well with the ν_{HB} predictions for the bare halide–acetylene complexes by Botschwina and coworkers [6,13]. Although the predictions tend to slightly underestimate the experimental frequencies of the Ar solvated complexes (by 5, 18, and 25 cm^{-1}, respectively), the agreement can be regarded as excellent.

The marginal effects of attached argon atoms on the vibrational properties of the core halide–acetylene complexes are consistent with infrared studies on the $X^- – H_2O \cdot Ar_n$ clusters ($X^- = Cl^-$, Br^-, I^-). In these systems, the halide is attached to the water molecule through a single hydrogen bond forming an asymmetric C_s structure. The argon induced vibrational band shift of the bound O–H stretching mode was found to be $\approx + 12 \ cm^{-1}$/Ar atom for $F^- – H_2O \cdot Ar_n$, $\approx -3 \ cm^{-1}$/Ar for $I^- – H_2O \cdot Ar_n$, and even less for $Cl^- – H_2O \cdot Ar_n$ [18].

At this stage, the structures of the $X^- – (C_2H_2) \cdot Ar_n$ complexes are not known. However, it seems likely that a linear, hydrogen-bonded $X^- – C_2H_2$ core is preserved in the Ar solvated complexes and that the Ar atom resides adjacent to the halide anion. While dispersion forces may encourage the Ar and C_2H_2 sub-units to congregate, this tendency will be counteracted by the interaction between the induced dipoles on the Ar atom and acetylene molecule, which will act to keep the sub-units apart. The potential energy surface along the coordinate corresponding to deformation of the angle between the $X^- – Ar$ and $X^- – HCCH$ bonds is expected to be soft, with the corresponding vibration possessing a very low frequency. Eventually, the structures of the argon-solvated halide–acetylene clusters and their vibrational modes may be elucidated through ab initio studies.

References

[1] P.S. Weiser, D.A. Wild, E.J. Bieske, J. Chem. Phys. 110 (1999) 9443.
[2] D.A. Wild, P.J. Milley, Z.M. Loh, P.S. Weiser, E.J. Bieske, Chem. Phys. Lett. 323 (2000) 49.
[3] D.A. Wild, P.J. Milley, Z.M. Loh, P.P. Wolynec, P.S. Weiser, E.J. Bieske, J. Chem. Phys. 113 (2000) 1075.
[4] P.S. Weiser, D.A. Wild, E.J. Bieske, Chem. Phys. Lett. 299 (1999) 303.
[5] M. Meuwly, P.P. Wolynec, E.J. Bieske, J. Chem. Phys. 116 (2002) 4948.
[6] P. Botschwina, R. Oswald, J. Chem. Phys. 117 (2002) 4800.
[7] M. Okumura, L.I. Yeh, J.D. Myers, Y.T. Lee, J. Chem. Phys. 85 (1986) 2328.
[8] P. Ayotte, G.H. Weddle, J. Kim, M.A. Johnson, J. Am. Chem. Soc. 120 (1998) 12361.
[9] P. Ayotte, J.A. Kelley, S.B. Nielsen, M.A. Johnson, Chem. Phys. Lett. 316 (2000) 455.
[10] P. Ayotte, G.H. Weddle, C.G. Bailey, M.A. Johnson, F. Vila, K.D. Jordan, J. Chem. Phys. 110 (1999) 6268.
[11] I. Yourshaw, Y. Zhao, D.M. Neumark, J. Chem. Phys. 105 (1996) 351.
[12] T. Lenzer, I. Yourshaw, M.R. Furlanetto, G. Reiser, D.M. Neumark, J. Chem. Phys. 110 (1999) 9578.
[13] P. Botschwina, H. Stoll, PCCP 3 (2001) 1965.
[14] J.E. Bartmess, in: P.J. Linstrom, W.G. Mallard (Eds.), Negative Ion Energetics Data, NIST Chemistry WebBook, NIST Standard Reference Database Number 69, National

Institute of Standards and Technology, Gaithersburg MD 20899, July 2001. Available from <http://webbook.nist.gov>.

[15] J.D.D. Martin, J.W. Hepburn, J. Chem. Phys. 109 (1998) 8139.

[16] C. Blondel, P. Cacciani, C. Delsart, R. Trainham, Phys. Rev. A 40 (1989) 3698.

[17] D. Hanstorp, M. Gustafsson, J. Phys. B 25 (1992) 1773.

[18] J.A. Kelley, J.M. Weber, K.M. Lisle, W.H. Robertson, P. Ayotte, M.A. Johnson, Chem. Phys. Lett. 327 (2000) 1.

[19] G. Herzberg, Molecular Spectra and Molecular Structure, Volume II, Infrared and Raman Spectra of Polyatomic Molecules, Krieger, Malabar, 1991.